Movement Analysis and Displacement Estimation of Human Lower Body by Inertial Sensors

Shuang Gong[a] and Qixing Ding

School of Chongqing University of Posts and Telecommunications, Chongqing 400065, China.

[a]xouxousun@163.com

Abstract

Human motion capture system (HMCS) becomes an important approach to make special effects movies, rehabilitation medical and other human-computer interaction activities. With the development of Micro-Electro-Mechanical System (MEMS), micro and low-energy inertial sensors become a new platform for human movement analysis. For the problem of the inertial HMCS cannot provide the real displacement of body, an estimation algorithm for human position based on support leg recognition is proposed. By establishing kinematics model of lower body, we get the model of human joint rotation angle and the position model of human skeletal movement. In this paper, the support leg and swing leg are identified by analyzing the acceleration value from foot. Then the displacement of body can be estimated by the forward kinematics principle. The proposed algorithm is tested on the W891E electric dividing head and humans. The results show that the RMES values of the estimated positon for different walking routes are 0.6m and 1.3m in straight and circular patterns

Keywords

Human Attitude Measurement, Kinematics Model, Support Leg Detection, Displacement Estimation

1. Introduction

The human motion capture system (HMCS) is used to record the human body movement position and process, and collect the motion information to simulate into the digital character by sensors distributed at the special locations on human body[1-2]. The cores of HMCS are physical positioning, rotation angle measurement, spatial positioning and other three-dimensional calculation methods[3].

With the development of inertial sensing technology and micro-electro-mechanical systems (MEMS), the HMCS with inertial sensors comes into being[4]. The inertial HMCS is composed of the attitude measuring units and the data processing units[5]. The attitude measuring units consist of an accelerometer, a gyroscope and a magnetometer, which are bound to a fixed position in the body to collect the inertial motion data of the bones and joints when the body moves, and the sensor data are transferred to the data processing units to be synthesized into human motion data[6].

Academic research field, domestic and foreign research institutes and universities have conduct academic and engineering researches in HMCS. P. Chen et al. proposed a human model by three-dimensional modeling[7-8]. The method is based on rigid body dynamics theory, which is used to control the virtual characters skeletal movement by inertial sensor data according to the movement characteristics human joints[9-10]. However, due to the defect of HMCS that the system is passive device without a reference position to the area at the beginning, so it becomes the biggest challenges for us to get a reference displacement by HMCS in space.

2. The Joint rotation angle model for human lower body

The model for human lower body is established as follows. We create a model for human lower body with seven bones and six joints. Seven bones are pelvis, left and right femurs, left and right tibias, left and right foot, and six joints were left and right hips, left and right knees, left and right ankles. The skeletal model and the skeletal chain of human lower body are shown in Fig.1.

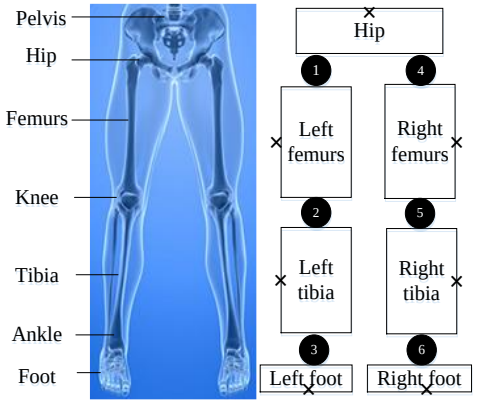

Fig.1 The skeletal model and the skeletal chain of human lower body

The system coordinate system is defined as follows. Assuming that the human body stand facing the north, the three axis of the reference coordinate system coincides with the geographic coordinate system as shown in Fig.2.

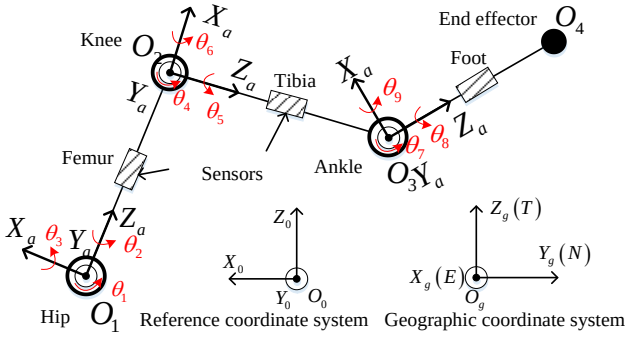

Fig.2 Schematic diagram of skeletal model coordinate system

When analyzing the movement of the whole skeletal chain, we can analyze the skeleton at all levels. We can get the attitude angles of the three joints in geographic coordinate system. The attitude angles of hip, knee and ankle are $\varphi_1,\theta_1,\psi_1$ and $\varphi_2,\theta_2,\psi_2$ and $\varphi_3,\theta_3,\psi_3$ respectively. We need to establish joint rotation angle model for human lower body to calculate the rotation angles of each node relative to the parent node $\theta_1,\theta_2,\theta_3$ and $\theta_4,\theta_5,\theta_6$ and $\theta_7,\theta_8,\theta_9$. The algorithm can be summarized as the following steps.

Step 1: The reference coordinate system is rotated $\varphi_0,\theta_0,\psi_0$ around the three axes of the geometric coordinate system, and the two coordinate system will be coincided. We can get the attitude transformation matrix R_g^0 from the geometric coordinate system to the reference coordinate system:

$$R_g^0=\begin{pmatrix}\cos\psi_0\cos\theta_0 & \cos\theta_0\sin\psi_0 & -\sin\theta_0\\ -\cos\varphi_0\sin\psi_0+\cos\psi_0\sin\theta_0\sin\varphi_0 & \cos\psi_0\cos\varphi_0+\sin\psi_0\sin\theta_0\sin\varphi_0 & \cos\theta_0\sin\varphi_0\\ \sin\psi_0\sin\varphi_0+\cos\psi_0\cos\varphi_0\sin\theta_0 & -\cos\psi_0\sin\varphi_0+\cos\varphi_0\sin\psi_0\sin\theta_0 & \cos\theta_0\cos\varphi_0\end{pmatrix} \quad (1)$$

And then we can get the attitude transformation matrix R_0^g from the reference coordinate system O_0 to the geometric coordinate system O_g, which is the inverse matrix of R_g^0:

$$R_0^g=\begin{pmatrix}g_{11} & g_{12} & g_{13}\\ g_{21} & g_{22} & g_{23}\\ g_{31} & g_{32} & g_{33}\end{pmatrix}=R(\varphi_0,\theta_0,\psi_0) \quad (2)$$

The homogeneous coordinate transformation matrix ${}_0^gT$ from the reference coordinate system to the geometric coordinate system can be written as follow:

$$ {}^{g}_{0}T = \begin{bmatrix} R_0^g & p_{0g} \\ 0 & 1 \end{bmatrix} \tag{3} $$

Step 2: Similarly, we can get the attitude transformation matrix R_1^g and the homogeneous coordinate transformation matrix ${}^{g}_{1}T$ from the hip joint coordinate system to the geometric coordinate system:

$$ \begin{aligned} R_1^g &= \begin{pmatrix} a_{11} & a_{12} & a_{13} \\ a_{21} & a_{22} & a_{23} \\ a_{31} & a_{32} & a_{33} \end{pmatrix} = R(\varphi_1, \theta_1, \psi_1) \\ {}^{g}_{1}T &= \begin{bmatrix} R_1^g & p_{1g} \\ 0 & 1 \end{bmatrix} \end{aligned} \tag{4} $$

Step 3: The projection from joint coordinate to the reference coordinate system can be seen as the reference coordinate system being rotated $\theta_1, \theta_2, \theta_3$ around the three axes of joint coordinate. Thus the attitude transformation matrix R_1^0 and the homogeneous coordinate transformation matrix ${}^{0}_{1}T$ from the hip joint coordinate system to the reference coordinate system:

$$ \begin{aligned} R_1^0 &= \begin{pmatrix} A_{11} & A_{12} & A_{13} \\ A_{21} & A_{22} & A_{23} \\ A_{31} & A_{32} & A_{33} \end{pmatrix} = R(\theta_1, \theta_2, \theta_3) \\ {}^{0}_{1}T &= \begin{bmatrix} R_1^0 & p_{10} \\ 0 & 1 \end{bmatrix} \end{aligned} \tag{5} $$

Step 4: The projection from joint coordinate to the geometric coordinate system can be divided into two rotation steps. Firstly the geometric coordinate system is rotated $\varphi_0, \theta_0, \psi_0$ around the three axes to the reference coordinate system, and then the coordinate system is rotated $\theta_1, \theta_2, \theta_3$ around the three axes to the final position. So we can get the following equation.

$$ {}^{g}_{1}T = {}^{g}_{0}T \, {}^{0}_{1}T \text{ , namely, } {}^{0}_{1}T = \left({}^{g}_{0}T \right)^{-1} {}^{g}_{1}T \tag{6} $$

Substitute Eq.3, Eq.4 and Eq.5 into Eq.6, we can get the follows.

$$ \begin{bmatrix} R_1^0 & p_{10} \\ 0 & 1 \end{bmatrix} = \begin{bmatrix} R_0^g & p_{0g} \\ 0 & 1 \end{bmatrix}^{-1} \begin{bmatrix} R_1^g & p_{1g} \\ 0 & 1 \end{bmatrix} = \begin{bmatrix} \left(R_0^g \right)^{-1} & \vdots \\ 0 & 1 \end{bmatrix} \begin{bmatrix} R_1^g & p_{1g} \\ 0 & 1 \end{bmatrix} = \begin{bmatrix} \left(R_0^g \right)^{-1} R_1^g & \vdots \\ 0 & 1 \end{bmatrix} \tag{7} $$

According to the determinant nature, the first element of the matrix on both sides of the equation is equal, so:

$$ R_1^0 = \left(R_0^g \right)^T R_1^g \tag{8} $$

Substitute Eq.2, Eq.4 and Eq.5 into Eq.8, we can get the following equations.

$$ \begin{aligned} A_{11} &= g_{11}a_{11} + g_{21}a_{21} + g_{31}a_{31} \\ A_{21} &= g_{12}a_{11} + g_{22}a_{21} + g_{32}a_{31} \\ A_{31} &= g_{13}a_{11} + g_{23}a_{21} + g_{33}a_{31} \\ A_{32} &= g_{13}a_{12} + g_{23}a_{22} + g_{33}a_{32} \\ A_{33} &= g_{13}a_{13} + g_{23}a_{23} + g_{33}a_{33} \end{aligned} \tag{9} $$

After operating the results can be obtained.

$$\theta_1 = \arctan\left(-\frac{A_{31}}{\sqrt{A_{32}^2 + A_{33}^2}}\right)$$
$$\theta_2 = \arctan\left(\frac{A_{21}}{A_{11}}\right) \tag{10}$$
$$\theta_2 = \arctan\left(\frac{A_{32}}{A_{33}}\right)$$

Similarly, according to the derivation of the above method, the rotation angles $\theta_4, \theta_5, \theta_6$ and $\theta_7, \theta_8, \theta_9$ of joints knee and ankle relative to their parent nodes can be obtained, respectively. The principle of the human joint angle rotation model can be shown in Fig.3.

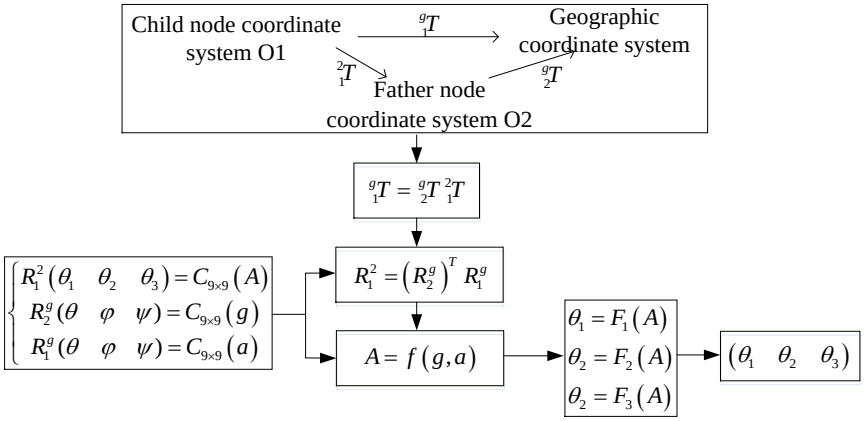

Fig.3 Principle of human joint angle rotation model

There are two kinds of states of legs when walking, one is the support period and the other is the swing period. In a complete walking cycle, the time of one leg support period and the swing period is about 3: 7. The process can be divided into three states. Process I: the left and right legs both are support legs. Process II: the left leg is swing and the right leg is supporting. Process III: this state is an opposite approach to process II.

In this paper, the Euclidean norm of the three axis accelerometer data is used to determine whether the leg is in the support or swing phase. According to the definition of Euclidean norm, we can calculate the three axis acceleration value of the sensors on the left and right feet.

$$Acc_{letf} = \sqrt{a_{x,left}^2 + a_{y,left}^2 + a_{z,left}^2}$$
$$Acc_{right} = \sqrt{a_{x,right}^2 + a_{y,right}^2 + a_{z,right}^2} \tag{11}$$

Due to the large fluctuations of the original data, which is not conducive to analyze the data. So we need to deal with the data by the Hamming Window Function Filter. The data after filtering is shown in Fig.4

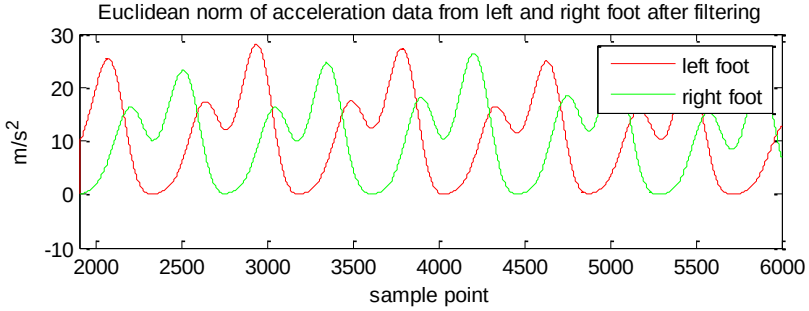

Fig.4 Euclidean norm of accelerometer data from left and right foot

3. Displacement estimation algorithm of the root node

According to the above, the rotation azimuth angles of the hip joints and the knee joints have been obtained, and the vector plane angles of the hip joints and knee joints can be calculated as follows:

$$\begin{aligned}\delta_{hip,t} &= \arccos\left(\frac{\left(Q_{tight,t}\otimes r_{tight,0}\otimes Q_{tight,t}^{-1}\right)_z}{r_{tight,t}}\right)\\ \delta_{knee,t} &= \arccos\left(\frac{\left(Q_{shin,t}\otimes r_{shin,0}\otimes Q_{shin,t}^{-1}\right)_z}{r_{shin,t}}\right)\end{aligned} \tag{12}$$

After getting the vector plane angles of the hip joints and knee joints, we can calculate the horizontal displacement of the hip and knee joints of the support leg in the course of walking respectively.

$$\begin{aligned}S_{Ship} &= L_{tight}\sin\left(\delta_{hip,t+\Delta t}\right)-L_{tight}\sin\left(\delta_{hip,t}\right)\\ S_{knee} &= L_{shin}\sin\left(\delta_{knee,t+\Delta t}\right)-L_{shin}\sin\left(\delta_{knee,t}\right)\end{aligned} \tag{13}$$

Therefore, the horizontal displacement of the root node during one time of walking is the sum of the horizontal displacement of the hip joint and knee joint:

$$S_{root} = S_{Ship} + S_{knee} \tag{14}$$

The attitude azimuth data Q_{root} measured by the sensor fixed on the root node (hip) can be used to determine the heading angle of the body in the reference coordinate system. And then according to the following formula, the displacement coordinates in the plane of the root node can be calculated.

$$\begin{aligned}S_{x,t+\Delta t} &= S_t + S_{root}\cdot\cos\left(\psi_{root}\right)\\ S_{y,t+\Delta t} &= S_t + S_{root}\cdot\sin\left(\psi_{root}\right)\end{aligned} \tag{15}$$

4. Experiment process and result analysis

4.1 Experiment platform

In order to verify the accuracy of the attitude measurement model proposed in this paper, the human lower leg is taken as an example to carry out experimental research and analysis. Simulation experiments are designed to verify the accuracy and reliability of the algorithm. Fig.5 shows the inertial sensor, which contains a sensor (MPU6050) including a tri-axis gyroscope and a tri-axis accelerometer, and a tri-axis magnetometer (HMC5883). Fig.6 shows the W891E electric dividing head.

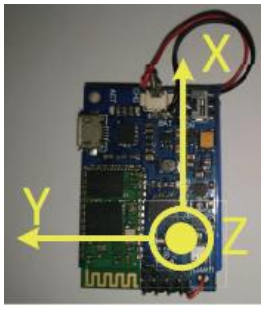

Fig.5 The inertial sensor unit

Fig.6 The W891E electric dividing head

4.2 Simulation Experiment Verification

According to the characteristics of the kick movement behavior, the root node module is fixed separately and does not rotate with the dividing head. The sensing units of the femur and tibia parts is vertically fixed on the dividing head base, the axis x of sensor unit is perpendicular to the dividing head base, and the axis z is straight up. The angles and ranges of the kicking leg are simulated by controlling the corner of the dividing head. The sketch of kicking is shown in Fig.7.

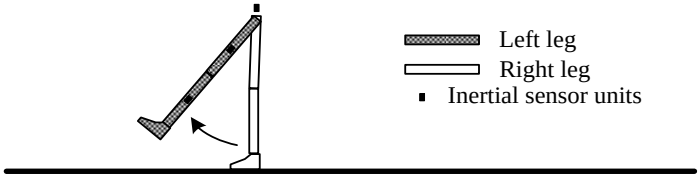

Fig.7 Sketch of kicking

The quantitative index for evaluating the kinematics model of the human body is to calculate the RMSE value of the attitude angles of the hip and knee joints with the reference value of the outputs of the dividing head. In this paper, we simulate the kicking angles of 30 degrees, 45 degrees and 60 degrees respectively for three times. The RMSE of all samples collected at each experiment is shown in Tab.1.

Tab.1 The azimuth RMSE of hip and knee of kicking movement (°)

No.	Hip			Knee		
	Roll	Pitch	Yaw	Roll	Pitch	Yaw
30°-1	1.8	0.5	1.6	1.3	0.6	1.2
30°-2	1.7	0.8	1.3	1.5	0.7	1.3
30°-3	1.7	0.6	1.4	1.5	0.8	1.5
45°-1	1.6	0.8	1.6	1.6	1.0	1.3
45°-2	1.1	1.0	1.0	1.8	1.2	1.2
45°-3	1.5	1.1	1.2	1.9	0.9	1.6
60°-1	2.0	0.9	1.8	1.6	0.8	1.5
60°-2	2.3	0.8	1.3	1.7	0.6	1.2
60°-3	2.2	0.6	1.7	1.4	0.5	1.2

The results show that the RMSE of the three angles of leg joints during kicking movement are lower than 2 degrees.

4.3 Verification of human root node displacement estimation

The subjects were asked to walk on the flat road surface, and the sensor data were collected in seven parts of human lower legs. In order to evaluate the accuracy of the estimation algorithm of the root node displacement, the location coordinates of the root node and the actual walking position are compared. In this paper, the straight line is tested, and the trajectory is shown in Fig.8.

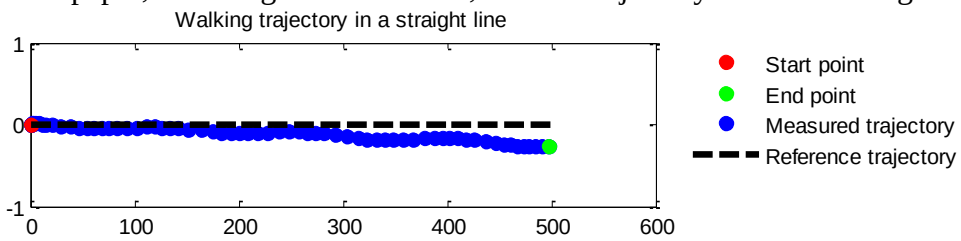

Fig.8 Walking trajectory in a straight line

The blue locus is the root node displacement trajectory calculated by the displacement estimation algorithm, and the black represents the reference trajectory. Fig.10 shows the displacement path of 50 meters along the runway, red point is the starting point, green point is the end point. The final displacement deviation is 0.5 meters compared with the black reference trajectory, and the root node displacement estimation accuracy is higher than 1%.

In order to verify the stability and universality of the algorithm, three testers were selected to test the walking line respectively. Each tester were asked to walk three times to collect data, simulate and analyze. The statistical results are shown in Tab.2. The results of the straight line test show that the

three testers were tested in nine times, and the errors were less than 1 meter, that is, the accuracy is higher than 1%.

Tab.2 RMSE of root node displacement estimation algorithm

No.	tester1		tester2		tester3	
	RMSE	accuracy	RMSE	accuracy	RMSE	accuracy
route1	0.5m	0.5%	0.6m	0.6%	0.7m	0.7%
route2	0.6m	0.6%	0.7m	0.7%	0.5m	0.5%
route3	0.6m	0.6%	0.9m	0.9%	0.9m	0.9%

5. Conclusion

For the HMCS can not accurately update the location of the root node coordinates, the algorithm of human motion displacement based on the support leg detection is proposed. Firstly, according to the Euclidean norm of accelerometer data of foot, the support leg and swing leg are identified and detected. Then the inverse kinematics process of the forward kinematics principle is used to solve the displacement of the root node, and finally the displacement coordinates of the root node are obtained. It is proved by experiments that the accuracy of the algorithm based on the support leg detection algorithm can meet the needs of the motion capture system, the root node displacement estimation accuracy is higher than 1%, and it is feasible and reliable.

References

[1] Ligorio G, Sabatini A M. A novel Kalman filter for human motion tracking with an inertial-based dynamic inclinometer[J]. IEEE Transactions on Biomedical Engineering, Vol. 62 (2015) No.8, p.2033-2043.

[2] Vondrak M, Sigal L, Jenkins O C. Dynamical simulation priors for human motion tracking[J]. IEEE transactions on pattern analysis and machine intelligence, Vol. 35 (2013) No.1, p.52-65.

[3] Wang Y, Wang L, Yang T, et al. Wearable and highly sensitive graphene strain sensors for human motion monitoring[J]. Advanced Functional Materials, Vol. 24 (2014) No.29, p. 4666 -4670.

[4] Clayton R B, Leshner G. The uncanny valley: The effects of rotoscope animation on motivational processing of depression drug messages[J]. Journal of Broadcasting & Electronic Media, Vol. 59 (2015) No.1, p.57-75.

[5] Bernard J, Wilhelm N, Krüger B, et al. Motionexplorer: Exploratory search in human motion capture data based on hierarchical aggregation[J]. IEEE transactions on visualization and computer graphics, Vol. 19 (2013) No.12, p. 2257-2266.

[6] Sarafianos N, Boteanu B, Ionescu B, et al. 3D Human Pose Estimation: A Review of the Literature and Analysis of Covariates[J]. Computer Vision & Image Understanding, Vol. 2016 (2016) No.152, p. 1-20.

[7] Demir U, Kocaoğlu S, Akdoğan E. Human impedance parameter estimation using artificial neural network for modelling physiotherapist motion[J]. Biocybernetics & Biomedical Engineering, Vol. 36 (2016) No.2, p. 318-326.

[8] Martins, José Manuel. 'Crows' vs. 'Avatar,' or: 3D vs. Total-Dimension Immersion[J]. Acta Universitatis Sapientiae, Film\s&\smedia Studies, Vol. 8 (2014) No.1, p. 79-96.

[9] Sigal L, Balan A O, Black M J. HumanEva: Synchronized Video and Motion Capture Dataset and Baseline Algorithm for Evaluation of Articulated Human Motion[J]. International Journal of Computer Vision, Vol. 87 (2010) No.1, p. 4-27.

[10] Shotton J, Sharp T, Kipman A, et al. Real-time human pose recognition in parts from single depth images[J]. Communications of the ACM, Vol. 56 (2013) No.1, p. 116-124.